

Accurate lattice geometrical parameters and bulk moduli from a semilocal density functional

Cite as: AIP Advances 8, 095209 (2018); <https://doi.org/10.1063/1.5050241>

Submitted: 26 March 2018 • Accepted: 13 August 2018 • Published Online: 11 September 2018

Yuxiang Mo, Hong Tang, Arun Bansil, et al.



View Online



Export Citation



CrossMark

ARTICLES YOU MAY BE INTERESTED IN

[A consistent and accurate ab initio parametrization of density functional dispersion correction \(DFT-D\) for the 94 elements H-Pu](#)

The Journal of Chemical Physics **132**, 154104 (2010); <https://doi.org/10.1063/1.3382344>

[Hybrid functionals based on a screened Coulomb potential](#)

The Journal of Chemical Physics **118**, 8207 (2003); <https://doi.org/10.1063/1.1564060>

[Rungs 1 to 4 of DFT Jacob's ladder: Extensive test on the lattice constant, bulk modulus, and cohesive energy of solids](#)

The Journal of Chemical Physics **144**, 204120 (2016); <https://doi.org/10.1063/1.4948636>



Accurate lattice geometrical parameters and bulk moduli from a semilocal density functional

Yuxiang Mo,¹ Hong Tang,¹ Arun Bansil,² and Jianmin Tao^{1,a}

¹Department of Physics, Temple University, Philadelphia, Pennsylvania 19122, USA

²Department of Physics, Northeastern University, Boston, Massachusetts 02115, USA

(Received 26 March 2018; accepted 13 August 2018; published online 11 September 2018)

Accurate prediction of lattice constants is very important in applications of density functional theory. In this work, we assess the efficacy of a non-empirical meta-generalized gradient approximation proposed by Tao and Mo (TM) by calculating the lattice constants as well as bulk moduli of 33 crystalline semiconductors within the TM scheme. We find that the TM functional is able to produce very accurate lattice constants, with a mean absolute error of 0.038 Å, and bulk moduli with a mean absolute error of 3.2 GPa, improving upon commonly-used semilocal density functionals, such as the LSDA, PBE, SOGGA, PBEsol, TPSS, M06L, and SCAN. The high computational efficiency and remarkable agreements with the corresponding experimental values suggest that the TM functional can be a very competitive candidate in electronic structure theory. We attribute the accuracy of the TM functional to be the result of its satisfaction of many exact or nearly-exact conditions related to the exchange-correlation energy and the associated hole, leading to an improved description of the short- as well as intermediate-range van der Waals interactions. © 2018 Author(s). All article content, except where otherwise noted, is licensed under a Creative Commons Attribution (CC BY) license (<http://creativecommons.org/licenses/by/4.0/>). <https://doi.org/10.1063/1.5050241>

I. INTRODUCTION

Kohn-Sham (KS) density functional theory¹ (DFT) is being used extensively for investigating electronic structures of wide classes of molecules and solids. The theory is successful in providing insights into electronic structures of materials with comparable accuracy but at a relatively cheap computational cost, compared to many-body approaches. Further progress toward higher accuracy and broader applicability of DFT relies on the development of improved approximations for the exchange-correlation energy functional, which is a key ingredient in the theory. The simplest approximation is the local spin-density approximation (LSDA),² which only invokes the local spin-densities in evaluating the exchange-correlation energy. The generalized-gradient approximations (GGAs)^{3–9} expand the variational freedom by including gradients of spin-densities as additional inputs. This allows the theory to satisfy more exact constraints and yield an improvement over the LSDA. The meta-GGAs^{10–12} further include Kohn-Sham orbital kinetic energy densities for determining the exchange-correlation energy. Due to the inclusion of the orbital kinetic energy density, a meta-GGA functional can further strengthen the slowly-varying condition by including the fourth-order gradient expansion in the exchange part, and at the same time makes a correlation functional be one-electron self-interaction free. Furthermore, the exchange part can be also constructed to be self-interaction free for hydrogen atom, a paradigm density in quantum chemistry. As a result, meta-GGA functionals are generally expected to achieve higher accuracy than GGAs. A number of density functionals have been developed along these lines in recent years and have led to improved predictions of ground state energies and related properties, and even excitation energies.^{13,14}

^aCorresponding author: jianmin.tao@temple.edu



Recently, Tao and Mo (TM) proposed a semilocal meta-GGA exchange-correlation functional,¹⁵ in which the exchange part was derived from a density matrix expansion, while the correlation part is based on the TPSS correlation with a modification in the low-density limit. The idea is that under a general coordinate transformation, the exchange hole becomes more localized. This localization makes the modeling of the exchange hole with a semilocal functional easier than the conventional exchange hole, which is fully nonlocal. The striking feature of this functional is that it not only satisfies the exact or nearly-exact constraints on the exchange-correlation energy, but also some important constraints on the underlying exchange-correlation hole. So, the starting point of the TM functional is different from many other meta-GGA functionals such as TPSS and SCAN, which were developed by satisfying the constraints on the exchange-correlation energy. As such, a comparative study of this density functional with other commonly-used functionals is highly desired.

Here, we assess the efficacy of the TM exchange-correlation functional by considering the equilibrium lattice constants and bulk moduli of 33 bulk crystalline semiconductors. Lattice constants are of fundamental importance as they drive the computation of all other physical properties of solids,^{16–18} while bulk moduli are the curvatures of the ground-state energies near the equilibrium state, which are also important. The set of solids considered in this study is as follows. (1) The common elemental semiconductors C (diamond), Si and Ge. (2) Binary semiconductors SiC, BP, BAs, AlP, AlAs, AlSb, β -GaN, GaP, GaAs, GaSb, InN, InP, InAs, InSb, ZnS, ZnSe, ZnTe, CdS, CdSe, CdTe, MgS, MgSe, MgTe, BaS, BaSe and BaTe. (3) Tetragonal and cubic PbTiO₃, and, (4) graphite and hexagonal boron nitride (h-BN). Regarding these choices of systems, elemental and binary semiconductors are interesting due to their applications in information technology and renewable energy. PbTiO₃ is a representative ferroelectric material, which also has many technological applications. Properties of PbTiO₃ are highly sensitive¹⁹ to lattice constant, and accurate prediction of its lattice constants in cubic and tetragonal phases has presented a challenge to DFT. Finally, we consider graphite and h-BN as exemplars of layered materials where the interlayer bonding is of weak van der Waals type, while there are strong intra-layer interactions resulting in covalent bonding. Although the bond lengths within the layers are given reasonably by many DFT-based methods, this is not the case when it comes to interlayer distances, because of the missing of long-range van der Waals (vdW) interactions. Our analysis will show that the TM functional can yield systematic improvements in the prediction of lattice constants of the diverse set of materials considered in this study.

II. COMPUTATIONAL METHOD

Calculations were performed with a locally modified version¹⁵ of Gaussian 09 program²⁰ using periodic boundary conditions.²¹ Pruned (99,590) grids were used in the evaluation of integrals. Dense k -point meshes were used for accurate evaluation of energies. They were adopted as follows: $10 \times 10 \times 10$ to $20 \times 20 \times 20$ for elemental and binary semiconductors; $12 \times 12 \times 10$ for tetragonal PbTiO₃; $12 \times 12 \times 12$ for cubic PbTiO₃; and $18 \times 18 \times 8$ for graphite and h-BN. Meshes with higher k -point densities were found to produce negligible differences.

We turn now to address our choices of basis sets for various materials investigated. These basis sets are taken from the literature as follows. For elemental and binary semiconductors, we adopted the modified 6-311G* basis set of Heyd *et al.*²² for light elements (B, C, N, Mg, Al, Si, P, S), and the small-core relativistic effective core potential with a double zeta valence basis set^{22,23} for heavier elements. For heavy Pb and Ti atoms in PbTiO₃, the basis set includes LANL effective core potential by Hay and Wadt²⁴ and the Gaussian-type functions by Piskunov *et al.*²⁵ The basis set by Catti *et al.*²⁶ was used for O atom. For the calculation of lattice constants of layered materials (graphite and h-BN), a relatively small basis set 6-31G(d) was used, in order to avoid high computational cost.

Ref. 27 has shown that the effect of basis size on lattice constants is fairly small. For example, for the lattice constant of silicon, PBE and TPSS yield 5.490 Å and 5.477 Å, respectively, with basis set 6-31G*; the corresponding results are 5.483 Å and 5.469 Å with a larger basis set 6-311G*, and 5.479 Å and 5.466 Å with the modified basis set m-6-311 G*. A larger basis set thus seems to favor a small shrinking in lattice constant. Given that the TM functional yields a mean error of

+0.034 Å in lattice constant (longer than experimental values, see Table I), and that slightly shorter lattice constants are expected by using the larger basis sets, we would expect the TM to generally lead to an improved systematic agreement with experimental results if larger basis sets were used in Tables I and II. Furthermore, the validity of our lattice constants evaluated with the choice of the basis set can be verified by excellent agreement with the plane wave-based VASP code²⁸ using ultrasoft

TABLE I. Comparison of equilibrium lattice constants (in Å) of 33 semiconductors calculated with different methods.^a Experimental values have been corrected for thermal effects as well as for zero-point energies (ZPE) as discussed in the text. The Strukturbericht symbols denote the types of crystal structures: diamond (A4), rock salt (B1), zinc blende (B3), and wurtzite (B4). Mean error (ME) and mean absolute error (MAE) are given, where the error is defined as the difference (theory-experiment). MAX and MIN are the maximum and minimum errors, respectively.

Solid		Expt.	LSDA	PBE	PBEsol	TPSS	SOGGA	M06L	SCAN	TM
C (A4)		3.555	3.537	3.579	3.561	3.579	3.556	3.560	3.555	3.558
Si (A4)		5.422	5.410	5.479	5.442	5.466	5.430	5.427	5.425	5.432
Ge (A4)		5.644	5.634	5.776	5.692	5.744	5.672	5.752	5.687	5.671
SiC (B3)		4.348	4.355	4.404	4.380	4.394	4.374	4.350	4.352	4.376
BP (B3)		4.527	4.509	4.567	4.540	4.566	4.528	4.535	4.521	4.536
BAs (B3)		4.764	4.750	4.829	4.788	4.821	4.774	4.805	4.779	4.776
AlP (B3)		5.450	5.436	5.508	5.472	5.497	5.461	5.452	5.478	5.467
AlAs (B3)		5.649	5.639	5.733	5.682	5.713	5.670	5.697	5.670	5.674
AlSb (B3)		6.126	6.079	6.188	6.146	6.172	6.131	6.189	6.173	6.141
β -GaN (B3)		4.523	4.476	4.569	4.519	4.552	4.510	4.544	4.524	4.526
GaP (B3)		5.441	5.418	5.534	5.468	5.522	5.452	5.498	5.457	5.468
GaAs (B3)		5.641	5.626	5.771	5.687	5.745	5.668	5.753	5.664	5.674
GaSb (B3)		6.086	6.043	6.208	6.111	6.183	6.092	6.211	6.117	6.100
InN (B4)	(a)	3.527	3.523	3.599	3.551	3.589	3.543	3.594		3.564
	(c)	5.679	5.684	5.807	5.801	5.765	5.787	5.867		5.747
InP (B3)		5.858	5.839	5.970	5.891	5.961	5.869	5.947	5.938	5.898
InAs (B3)		6.048	6.038	6.195	6.099	6.170	6.078	6.205	6.122	6.093
InSb (B3)		6.473	6.430	6.608	6.501	6.585	6.489	6.644	6.545	6.500
ZnS (B3)		5.399	5.319	5.467	5.383	5.465	5.367	5.448	5.370	5.407
ZnSe (B3)		5.658	5.588	5.751	5.657	5.736	5.638	5.756	5.652	5.668
ZnTe (B3)		6.079	6.017	6.195	6.089	6.174	6.064	6.235	6.077	6.096
CdS (B3)		5.808	5.776	5.934	5.844	5.944	5.825	5.942	5.856	5.879
CdSe (B3)		6.042	6.025	6.210	6.098	6.195	6.075	6.249	6.100	6.121
CdTe (B3)		6.470	6.422	6.626	6.502	6.610	6.478	6.709	6.521	6.524
MgS (B3)		5.612	5.618	5.721	5.676	5.719	5.665	5.649	5.634	5.681
MgSe (B1)		5.375	5.417	5.532	5.477	5.520	5.458	5.520	5.454	5.483
MgTe (B3)		6.410	6.381	6.517	6.432	6.517	6.419	6.478	6.452	6.442
BaS (B1)		6.364	6.303	6.436	6.351	6.433	6.330	6.422	6.441	6.402
BaSe (B1)		6.570	6.517	6.671	6.577	6.659	6.556	6.694	6.659	6.631
BaTe (B1)		6.982	6.897	7.062	6.919	7.062	6.894	7.068	7.071	6.985
PbTiO ₃ tetragonal	(a)	3.878	3.872	3.845	3.861	3.884	3.869	3.906		3.895
	(c)	4.174	4.031	4.612	4.236	4.459	4.139	4.170		4.170
PbTiO ₃ cubic		3.911	3.894	3.958	3.921	3.957	3.913	3.950		3.936
Graphite	(a)	2.459	2.448	2.475	2.468	2.474	2.467	2.462	2.45	2.468
	(c)	6.672	6.582	7.290	7.157	7.266	7.125	6.691	6.86	6.954
h-BN	(a)	2.504	2.481	2.518	2.511	2.518	2.510	2.502	2.5	2.512
	(c)	6.652	5.895	7.266	6.981	8.109	6.958	6.540	6.84	6.598
ME			-0.051	0.125	0.046	0.134	0.028	0.071	0.042	0.034
MAE			0.054	0.127	0.052	0.134	0.043	0.078	0.045	0.038
RMS			0.132	0.186	0.104	0.275	0.096	0.101	0.065	0.061
MAX			0.042	0.618	0.485	1.457	0.453	0.239	0.188	0.282
MIN			-0.757	-0.033	-0.063	0.006	-0.088	-0.112	-0.029	-0.054

^aThe PBE, PBEsol, TPSS, SOGGA, and M06-L results for PbTiO₃ (tetragonal and cubic), graphite, and hBN are from Ref. 31. The LSDA results are from Ref. 32 for PbTiO₃ (tetragonal and cubic), Ref. 33 for graphite and Ref. 34 for h-BN. For other semiconductors, lattice constants predicted by the LSDA, PBE, PBEsol, TPSS, SOGGA, and M06-L are from Ref. 30. The results of graphite and h-BN from SCAN are from Ref. 35 and other results from SCAN are from Ref. 36. The experimental values are from Ref. 31 for the PbTiO₃ (tetragonal and cubic), graphite and h-BN, and from Ref. 30 for all other semiconductors, and have been corrected for zero point energy (ZPE), as described in Ref. 30.

TABLE II. Calculated bulk moduli (GPa) for a set of 27 semiconductors using different DFT methods are compared with the corresponding experimental values. The Strukturbericht symbols denote the types of crystal structures: diamond (A4), rock salt (B1), and zinc blende (B3). ME is mean error and MAE is mean absolute error. MAX and MIN are the maximum and minimum errors, respectively.

Solid	Expt.	LSDA	PBE	TPSS	PBEsol	SCAN	TM
C (A4)	443	458.0	426	421	450	461.4	442.4
Si (A4)	99.2	95.6	89	91.9	94.2	98.7	97.1
Ge (A4)	75.8	75.9	63.0	66.4	68.1	71.4	72.5
SiC (B3)	225	225	209	213	218.0	225.7	220.0
BP (B3)	173	176	162	158	173.4	166.5	171.5
BAs (B3)	148	146	131		141		141.1
AlP (B3)	86	89.9	82.6	84.9	90.5	90.7	89.3
AlAs (B3)	82	75.5	67.0	70.3	78.7	75.5	75.2
AlSb (B3)	58.2	56.4	50.4		54.2		59.4
β -GaN (B3)	190	204	173	190	182.8	210.2	207.1
GaP (B3)	88	90.6	77.0	81.3	85.9	90.7	89.2
GaAs (B3)	75.6	81.3	68.1	70.1	69.1	73.3	78.6
GaSb (B3)	57	49.4	41.3	42.8	46.2		56.4
InP (B3)	73	71.0	59.5	60.0	66.7		68.2
InAs (B3)	60	60.0	48.5	50.0	55.6		57.9
InSb (B3)	47	46.4	36.9	37.9	42.8		47.3
MgS (B3)	78.9	84.0	74.4	77	60.9		79.8
MgSe (B1)	62.8	74.8	68.4				63.4
ZnS (B3)	76.9	88.0	70		79.1		77.5
ZnSe (B3)	62.5	70.4	57.3		66.7		64.6
ZnTe (B3)	51	54.9	43.2		51.6		51.3
CdS (B3)	62	64.3	52.9				57.5
CdSe (B3)	53	57.9	44.5				50.8
CdTe (B3)	42	48.2	34.6		42.3		41.5
BaS (B1)	39.4	46.3	38.5				47.5
BaSe (B1)	43.4	48.6	37.5				38.8
BaTe (B1)	29.4	37.4	31.8				31.0
ME		3.5	-9.1	-9.3	-3.5	2.7	-0.2
MAE		5.3	9.7	9.3	5.3	6.7	3.2
MAX		15	5.6	0	7	20.2	17.1
MIN		-7.6	-17	-22	-18	-6.5	-6.9

potential. For example, the lattice constant using Gaussian 09 with the above basis set is 4.376 Å (this work) for SiC solid, while the lattice constant of SiC from the VASP code is 4.380 Å. The discrepancy is only 0.004 Å. Therefore, the accuracy of the TM functional is quite robust and can be compared with those of other functionals in the literature. (Except for M06L in which Gaussian code with the same basis set was used, the lattice constants of all other functionals are evaluated with VASP code and therefore have no basis set issue). We use mean error (ME) and mean absolute error (MAE) to statistically characterize the accuracy of our theoretical predictions, where the error is defined as the difference between theory and experiment (theory-experiment) for various computed quantities. Maximum and minimum errors in the series of materials considered are also given in Tables I and II

III. RESULTS AND DISCUSSION

A. Lattice constants

Table I compares the equilibrium lattice constants of 33 semiconductors calculated using the TM functional with the corresponding experimental results, which have been extrapolated to 0 K using the approach discussed in Refs. 27 and 29. The zero-point anharmonic contributions were then removed from these experimental values along the lines discussed in Ref. 30. Results for lattice constants based on other functionals are taken as follows. The PBE, PBEsol, TPSS, SOGGA, and

M06-L results for PbTiO₃ (tetragonal and cubic), graphite, and hBN are from Ref. 31. The LSDA results are from Ref. 32 for PbTiO₃ (tetragonal and cubic), Ref. 33 for graphite and Ref. 34 for h-BN. For other semiconductors, lattice constants predicted by the LSDA, PBE, PBEsol, TPSS, SOGGA, and M06-L are from Ref. 30. The lattice constants for the SCAN functional¹² are from Ref. 35, except for those of graphite and h-BN, which are taken from Ref. 36.

The MAEs for different functionals are compared in Fig. 1. Similar to other functionals (excepting LSDA), the TM functional generally overestimates lattice constants with the exception of the *c* value in tetragonal PbTiO₃ and h-BN. The TM based lattice constants show a trend that the error increases as we go to heavier elements for elemental semiconductors or, in the case of binary semiconductors, the electron acceptor element is replaced by a heavier isoelectronic element. For example, the error in the TM lattice constants (theory-experiment) increases from 0.003 Å in C, to 0.010 Å in Si, and to 0.027 Å in Ge. Similarly, the error is 0.009 Å in BP but increases to 0.012 Å in BAs. However, this trend reverses when we reach Group V of the periodic table involving Sb and Te. The Zn series seems to be an exception in that the errors increase only slightly from 0.008 Å in ZnS to 0.010 Å in ZnSe, and to 0.017 Å in ZnTe. A similar trend is also seen with respect to the electron donor elements, although the reversal in the trend takes place in Group VI of the periodic table. For example, the error is 0.069 Å in MgS and 0.038 Å in BaS.

The TM functional predicts the value of the *c* lattice constant in tetragonal PbTiO₃ of 4.170 Å, which ties with the M06L result, and compares very well with the experimental value of 4.174 Å. For the lattice constant of cubic PbTiO₃, the TM functional is somewhat less accurate than LDA, PBEsol, and SOGGA, but more accurate than PBE, TPSS, and M06L. Notably, graphite and h-BN are layered materials, which are held together by van de Waals (vdW) forces.³⁷⁻³⁹ These long-range vdW interactions cannot be fully captured by a semilocal density functional, and have presented a well-known challenge for conventional density functionals. For graphite, the TM functional yields an interlayer distance of 6.954 Å, which is less accurate than LSDA and M06L but more accurate than the other density functionals considered. When it comes to h-BN, the TM-based interlayer distance is 6.598 Å, with an absolute error of 0.054 Å, which is only half of that for M06L (0.112 Å) and 1/6 to 1/27 of errors from other density functionals. The smaller error with the TM functional for the lattice constants of layered materials suggests that this functional provides an improved description of the short-and intermediate-range vdW interactions at equilibrium state, even though the long-range part is still missing. Overall, the TM functional is seen in Table I and Fig. 1 to exhibit the highest accuracy among all the functionals considered with MAE of only 0.038 Å, which is 12% smaller than SOGGA (MAE = 0.043 Å), 16% smaller than SCAN (MAE=0.045), 27% smaller than PBEsol (MAE = 0.052 Å), 30% smaller than LSDA (MAE = 0.054 Å), and much smaller than M06L (MAE = 0.078 Å), PBE (MAE = 0.127 Å), and TPSS (MAE = 0.134 Å). The TM functional

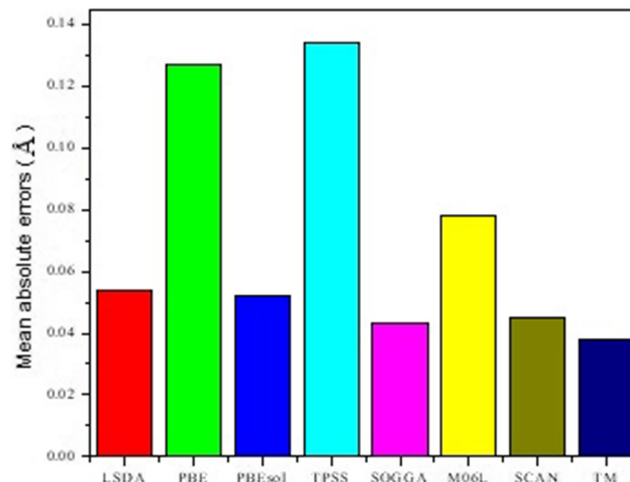


FIG. 1. Mean absolute errors are shown in the form of a bar chart from Table I for the different functionals considered.

has a root mean square (RMS) error of 0.061 Å, 6% smaller than SCAN (RMS = 0.065), 36% smaller than SOGGA (RMS = 0.096 Å) and much smaller than M06L (RMS = 0.101 Å), PBEsol (RMS = 0.104 Å), LSDA (RMS = 0.132 Å), PBE (RMS = 0.186 Å), and TPSS (RMS = 0.275 Å). The small value of the RMS error for TM speaks to its superior predictive capabilities with regard to the lattice constant. We normally expect a tradeoff between the performances of a density functional with respect to geometry and energetics, such as PBEsol. It is notable, therefore, that the TM functional not only yields accurate lattice constants, but that it also simultaneously provides accurate energetics of solids and surfaces,⁴⁰ and bond length and energetics of molecules.⁴¹ We attribute this excellent accuracy in lattice constants to the improved short-range description of the TM functional, due to the inclusion of more van der Waals interactions via the de-enhancement of the exchange-correlation energy in some regions.

B. Bulk moduli

The bulk modulus B_0 of a substance, which measures resistance to compression, is defined as

$$B_0 = - \left. \frac{dP}{dv} \right|_{v=v_0} = v \left. \frac{d^2\varepsilon}{dv^2} \right|_{v=v_0}, \quad (1)$$

where v is the volume per conventional unit cell, v_0 is the equilibrium value, ε is the bonding energy per conventional unit cell (tends to zero as $v \rightarrow \infty$), and P is the pressure. The bulk modulus, which can be calculated from the equation of state (EOS),⁴²⁻⁴⁴ involves the curvature of the energy vs volume curve, and thus it plays an important role in the energetics of the material. In this connection, we first computed total energies for at least ten different lattice volumes, which ranged from -5% to +5% of the equilibrium lattice volume. In principle, all EOS (e.g., Birch-Murnaghan,⁴³ Vinet⁴⁴ or a direct computation from derivatives) should yield the same bulk modulus. Here, we chose the stabilized jellium EOS,⁴² and fitted our computed values to those of the stabilized jellium EOS

$$\varepsilon(x) = \frac{a}{x^3} + \frac{b}{x^2} + \frac{c}{x} + d, \quad (2)$$

where $x = (v/v_0)^{1/3}$ is the compression ratio. The bulk modulus B_0 is then obtained by solving the following equations

$$a = \frac{9}{2} B_0 v_0 (B_1 - 3), \quad (3)$$

$$b = \frac{9}{2} B_0 v_0 (10 - 3B_1), \quad (4)$$

$$c = \frac{-9}{2} B_0 v_0 (11 - 3B_1). \quad (5)$$

Here, B_1 is the first derivative of the bulk modulus with respect to pressure at equilibrium.

The TM-based bulk moduli for a group of 27 semiconductors are compared in Table II with the corresponding experimental results. For BP, AIP, AlAs, GaN, GaP, and MgS, the LSDA and PBE values are from Ref. 45, and the PBEsol values are from Ref. 46. The LSDA, PBE, TPSS and PBEsol values for InP, InAs and InSb are from Ref. 17. The TPSS values for AIP and AlAs are from Ref. 36 and for BP, β -GaN and GaP are from Ref. 47. The results from SCAN are from Ref. 36. The LSDA, PBE, and TPSS values of C, Si, Ge, SiC, and GaAs are from Ref. 47. The TPSS value of MgS is from Ref. 48. The PBEsol values of C, Si, Ge, SiC and GaAs are from Ref. 49. The LSDA, PBE, TPSS and PBEsol values of GaSb are from Ref. 50. The LSDA and PBE values of ZnS and ZnSe are from Ref. 51. The LSDA and PBE values of BAs are from Ref. 52. The LSDA, PBE and PBEsol values of AlSb are from Ref. 53. The PBE values of ZnTe and CdTe are from Ref. 54. The PBE values of CdS and CdSe are from Ref. 55. The LSDA values of ZnTe, CdTe, CdS and CdSe are from Ref. 56. The PBEsol values of BAs, ZnS, ZnSe, ZnTe, and CdTe are from Ref. 57. The LDA and PBE values of MgSe are from Ref. 58. The LDA value of BaS is from Ref. 59 and for BaSe is from Ref. 60. The PBE value for BaS and BaSe is from Ref. 61. The LDA and PBE values for BaTe are from Ref. 62. The experimental data are from the following references: BaS,⁶³ BaSe,⁶⁴ BaTe,⁶⁵ C,⁶⁶ Si,⁶⁷ Ge,⁶⁷ SiC,⁶⁸ BP,⁶⁹ BAs,⁵⁷ AIP,⁷⁰ AlAs,⁷⁰ AlSb,⁵³ InP,¹⁷ InAs,¹⁷ InSb,¹⁷ GaN,⁷¹ GaP,⁷⁰ GaAs,⁶⁷ GaSb,⁵⁰ MgSe,⁵⁸ MgS,⁷² ZnS,⁷³ ZnSe,⁷³ ZnTe,⁷³ CdS,⁷³ CdSe,⁷³

and CdTe.⁷³ It can be seen from Table II that the TM functional predicts the most accurate bulk moduli with MAE=3.2GPa for the group of semiconductors considered here. The TM functional (ME = -0.2GPa), like all other functionals (except for the LSDA and SCAN), tends to underestimate the bulk moduli, while the LSDA and SCAN overestimate the bulk moduli with ME=3.5 GPa and 2.7 GPa, respectively. Since SCAN can also give accurate description of the short- and intermediate-range vdW interactions, as shown by its accurate lattice constants in Table I, we can conclude that bulk moduli are not sensitive to the vdW interactions. This conclusion is consistent with the findings of a recent work,⁷⁴ in which it was found that MAE of the bulk moduli of PBE+D3 is almost the same as that of PBE.

IV. CONCLUSION

In conclusion, we have assessed the accuracy of the nonempirical TM functional by computing equilibrium lattice constants of a group of 33 semiconducting crystals; bulk moduli for 27 of these crystals were also evaluated. The TM-based results for lattice constants and bulk moduli are compared and contrasted with the corresponding experimental values as well as the results from many commonly-used density functionals in the literature. Our analysis shows clearly that the TM functional is most accurate with respect to both lattice constants and bulk moduli, and exhibits the smallest mean absolute error among the density functionals considered. The good performance of the TM functional reflects the effects of many exact constraints on the exchange-correlation energy and the associated hole, which are built into the TM functional, such as those related to the slowly-varying density regime and the low-density limit. As a result, the TM functional also gives an improved description of the short- as well as intermediate-range vdW interactions. We conclude that the TM functional is a competitive candidate for addressing the ground state properties of semiconductors.

ACKNOWLEDGMENTS

YM acknowledges support from NSF under Grant no. CHE-1640584. JT and HT acknowledge support from the DOE office of science, Basic Energy Science (BES), under grant No. DE-SC0018194. JT also acknowledges support from Temple start-up via John Perdew. YM, HT, and JT acknowledge computational support from the HPC of Temple University and NERSC of DOE. The work at Northeastern University was supported by the US Department of Energy (DOE), Office of Science, Basic Energy Sciences grant number DE-FG02-07ER46352 (core research), and benefited from Northeastern University's Advanced Scientific Computation Center (ASCC), the NERSC Supercomputing Center through DOE grant number DE-AC02-05CH11231, and support (testing the efficacy of various exchange-correlation functionals) from the DOE EFRC: Center for the Computational Design of Functional Layered Materials (CCDM) under DE-SC0012575.

- ¹ W. Kohn and L. J. Sham, *Phys. Rev.* **140**, A1133 (1965).
- ² S. H. Vosko, L. Wilk, and M. Nusair, *Can. J. Phys.* **58**, 1200 (1980).
- ³ J. P. Perdew, *Phys. Rev. B* **33**, 8822 (1986).
- ⁴ C. Lee, W. Yang, and R. G. Parr, *Phys. Rev. B* **37**, 785 (1988).
- ⁵ R. H. Hertwig and W. Koch, *Chem. Phys. Lett.* **268**, 345 (1997).
- ⁶ J. P. Perdew, J. A. Chevary, S. H. Vosko, K. A. Jackson, M. R. Pederson, D. J. Singh, and C. Fiolhais, *Phys. Rev. B* **46**, 6671 (1992).
- ⁷ J. P. Perdew, K. Burke, and M. Ernzerhof, *Phys. Rev. Lett.* **77**, 3865 (1996).
- ⁸ M. Ernzerhof and G. E. Scuseria, *J. Chem. Phys.* **110**, 5029 (1999).
- ⁹ A. D. Boese and N. C. Handy, *J. Chem. Phys.* **114**, 5497 (2001).
- ¹⁰ J. Tao, J. P. Perdew, V. N. Staroverov, and G. E. Scuseria, *Phys. Rev. Lett.* **91**, 146401 (2003).
- ¹¹ Y. Zhao and D. G. Truhlar, *J. Chem. Phys.* **125**, 194101 (2006).
- ¹² J. Sun, A. Ruzsinszky, and J. P. Perdew, *Phys. Rev. Lett.* **115**, 036402 (2015).
- ¹³ S. S. Leang, F. Zaharieiev, and M. S. Gordon, *JCP* **136**, 104101 (2012).
- ¹⁴ G. Tian, Y. Mo, and J. Tao, *JCP* **146**, 234102 (2017).
- ¹⁵ J. Tao and Y. Mo, *Phys. Rev. Lett.* **117**, 073001 (2016).
- ¹⁶ Y. Fang, B. Xiao, J. Tao, J. Sun, and J. P. Perdew, *Phys. Rev. B* **87**, 214101 (2013).
- ¹⁷ F. Tran, J. Stelzl, and P. Blaha, *J. Chem. Phys.* **144**, 204120 (2016).
- ¹⁸ J. Tao, F. Zheng, J. Gebhardt, J. P. Perdew, and A. M. Rappe, *Phys. Rev. Mater.* **1**, 020802(R) (2017).
- ¹⁹ W. A. Al-Saidi and A. M. Rappe, *Phys. Rev. B* **82**, 155304 (2010).

- ²⁰ M. J. Frisch *et al.*, Gaussian 09, Revision A.02 (Gaussian, Inc., Wallingford CT, 2009).
- ²¹ K. N. Kudin and G. E. Scuseria, *Phys. Rev. B* **61**, 16440 (2000).
- ²² J. Heyd, J. E. Peralta, G. E. Scuseria, and R. L. Martin, *J. Chem. Phys.* **123**, 174101 (2005).
- ²³ B. Metz, H. Stoll, and M. Dolg, *J. Chem. Phys.* **113**, 2563 (2000).
- ²⁴ P. J. Hay and W. R. Wadt, *J. Chem. Phys.* **82**, 299 (1985).
- ²⁵ S. Piskunov, E. Heifets, R. I. Eglitis, and G. Borstel, *Comput. Mater. Sci.* **29**, 165 (2004).
- ²⁶ M. Catti, G. Valerio, R. Dovesi, and M. Causà, *Phys. Rev. B* **49**, 14179 (1994).
- ²⁷ J. Heyd, J. E. Peralta, G. E. Scuseria, and R. L. Martin, *J. Chem. Phys.* **123**, 174101 (2005).
- ²⁸ G. Kresse and J. Furthmüller, "Efficient iterative schemes for ab initio total-energy calculations using a plane-wave basis set," *Phys. Rev. B* **54**, 11169 (1996).
- ²⁹ M. J. Lucero, T. M. Henderson, and G. E. Scuseria, *J. Phys.: Condens. Matter* **24**, 145504 (2012).
- ³⁰ R. Peverati and D. G. Truhlar, *J. Chem. Phys.* **136**, 134704 (2012).
- ³¹ Y. Zhao and D. G. Truhlar, *J. Chem. Phys.* **128**, 184109 (2008).
- ³² D. I. Bilc, R. Orlando, R. Shaltaf, G.-M. Rignanese, J. Íñiguez, and P. Ghosez, *Phys. Rev. B* **77**, 165107 (2008).
- ³³ N. Ooi, A. Rairkar, and J. B. Adams, *Carbon* **44**, 231 (2006).
- ³⁴ N. Ooi, V. Rajan, J. Gottlieb, Y. Catherine, and J. B. Adams, *Model. Simul. Mater. Sci. Eng.* **14**, 515 (2006).
- ³⁵ H. Peng, Z. Yang, J. P. Perdew, and J. Sun, *Phys. Rev. X* **6**, 041005 (2016).
- ³⁶ S. Jana, A. Patra, and P. Samal, [arXiv:1802.05185v1](https://arxiv.org/abs/1802.05185v1), (2018).
- ³⁷ J. Klimeš and A. Michaelides, *J. Chem. Phys.* **137**, 120901 (2012).
- ³⁸ K. Berland, V. R. Cooper, K. Lee, E. Schröder, T. Thonhauser, P. Hyldgaard, and B. I. Lundqvist, *Rep. Prog. Phys.* **78**, 066501 (2015).
- ³⁹ S. Grimme, A. Hansen, J. G. Brandenburg, and C. Bannwarth, *Chem. Rev.* **116**, 5105 (2016).
- ⁴⁰ Y. Mo, R. Car, V. N. Staroverov, G. E. Scuseria, and J. Tao, *Phys. Rev. B* **95**, 035118 (2017).
- ⁴¹ Y. Mo, G. Tian, R. Car, V. N. Staroverov, G. E. Scuseria, and J. Tao, *J. Chem. Phys.* **145**, 234306 (2016).
- ⁴² A. B. Alchagirov, J. P. Perdew, J. C. Boettger, R. C. Albers, and C. Fiolhais, *Phys. Rev. B* **63**, 224115 (2001).
- ⁴³ F. Birch, *Phys. Rev.* **71**, 809 (1947).
- ⁴⁴ P. Vinet, J. H. Rose, J. Ferrante, and J. R. Smith, *J. Phys.: Condens. Matter* **1**, 1941 (1989).
- ⁴⁵ F. Tran, R. Laskowski, P. Blaha, and K. Schwarz, *Phys. Rev. B* **75**, 115131 (2007).
- ⁴⁶ P. Pernot, B. Civalieri, D. Presti, and A. Savin, *J. Phys. Chem. A* **119**, 5288 (2015).
- ⁴⁷ J. Heyd and G. E. Scuseria, *J. Chem. Phys.* **121**, 1187 (2004).
- ⁴⁸ V. N. Staroverov, G. E. Scuseria, J. Tao, and J. P. Perdew, *Phys. Rev. B* **69**, 075102 (2004); **78**, 239907(E) (2008).
- ⁴⁹ G. I. Csonka, J. P. Perdew, A. Ruzsinszky, P. H. T. Philipsen, S. Lebegue, J. Paier, O. A. Vydrov, and J. G. Angyan, *Phys. Rev. B* **79**, 155107 (2009).
- ⁵⁰ E.-E. Castaño-González, N. Seña, V. Mendoza-Estrada, R. González-Hernández, A. Dussan, and F. Mesa, *Semiconductors* **50**, 1280 (2016).
- ⁵¹ S. Bendaif, A. Boumazza, O. Nemiri, K. Boubendira, H. Meradji, S. Ghemid, and F. E. Haj Hassan, *Bull. Mater. Sci.* **38**, 365 (2015).
- ⁵² R. Mohammad and S. Katircioglu, *J. Alloys Compd.* **485**, 687 (2009).
- ⁵³ H. Salehi, H. Allah Bادهيann, and M. Farbod, *Mater. Sci. Semi. Proc.* **26**, 477 (2014).
- ⁵⁴ J. G. Collins, G. K. White, J. A. Birch, and T. F. Smith, *J. Phys. C: Sol. Stat. Phys.* **13**, 1649 (1980).
- ⁵⁵ S. Sarkar, S. Pal, P. Sarkar, A. L. Rosa, and T. Frauenheim, *J. Chem. Theory Comput.* **7**, 2262 (2011).
- ⁵⁶ G. Zhang, *Understanding the role of van der Waals forces in solids from first principles*, Dissertation, Free university of Berlin, 2014.
- ⁵⁷ P. Pernot, B. Civalieri, D. Presti, and A. Savin, *J. Phys. Chem. A* **119**, 5288 (2015).
- ⁵⁸ D. Rached, N. Benkhetto, B. Soudini, B. Abbar, N. Sekkal, and M. Driz, *Phys. Stat. Sol.(b)* **240**, 565 (2003).
- ⁵⁹ M. Ameri, K. Boudia, A. Rabhi, S. Benaissa, Y. Al-Douri, A. Rais, and D. Hachemane, *Mater. Sci. Appl.* **3**, 861 (2012).
- ⁶⁰ S. Wei and H. Krakauer, *Phys. Rev. Lett.* **55**, 1200 (1985).
- ⁶¹ M. Ameri, A. Touia, H. Khachai, Z. Mahdjoub, M. Z. Chekroun, and A. Slamani, *Mater. Sci. Appl.* **3**, 612 (2012).
- ⁶² H. Akbarzadeh, M. Dadsetani, and M. Mehrani, *Comput. Mater. Sci.* **17**, 81 (2000).
- ⁶³ S. Drablia, H. Meradji, S. Ghemid, G. Nouet, and F. El. H. Hassan, *Comput. Mater. Sci.* **46**, 376 (2009).
- ⁶⁴ T. A. Gryzbowski and A. L. Ruoff, *Phys. Rev. B* **27**, 6502 (1983).
- ⁶⁵ A. Jayaraman, A. K. Singh, A. Chatterjee, and S. U. Devi, *Phys. Rev. B* **9**, 2513 (1974).
- ⁶⁶ M. Levinshtein, S. Rumyantsev, and M. Shur, *Handbook Series on Semiconductor Parameters* (World Scientific, Singapore, 1996).
- ⁶⁷ K.-H. Hellwege, *Landolt-Bornstein, New Series, Group III* (Springer, Berlin, Germany, 1966).
- ⁶⁸ W. R. L. Lambrecht, B. Segall, M. Methfessel, and M. van Schilfgaarde, *Phys. Rev. B* **44**, 3685 (1991).
- ⁶⁹ S. Kalvoda, B. Paulus, P. Fulde, and H. Stoll, *Phys. Rev. B* **55**, 4027 (1997).
- ⁷⁰ D. Bimberg, R. Blachnik, M. Cardona, P. J. Dean, T. Grave, G. Harbeke, K. Hübner, U. Kaufmann, W. Kress, O. Madelung, W. von Münch, U. Rossler, J. Schneider, M. Schulz, and M. S. Skolnick, *Semiconductors: Physics of Group IV Elements and III-V Compounds* (Springer-Verlag, Berlin, Germany, 1982).
- ⁷¹ H. M. Tütüncü, S. Bağcı, G. P. Srivastava, A. T. Albudak, and G. Uğur, *Phys. Rev. B* **71**, 195309 (2005).
- ⁷² S. M. Peiris, A. J. Campbell, and D. L. Heinz, *J. Phys. Chem. Solids* **55**, 413 (1994).
- ⁷³ M. L. Cohen, *Phys. Rev. B* **32**, 7988 (1985).
- ⁷⁴ H. Tang and J. Tao, *Mater. Res. Express* **5**, 076302 (2018).